Encoding in a network of sparsely connected spiking neurons : application to locust olfaction

Etienne Hugues [*] Dominique Martinez

LORIA-INRIA, Nancy, France

Abstract

Experiments in the locust antennal lobe have revealed that during odor stimulation an oscillation appears together with an odor-specific transient synchronization of the projecting excitatory cells. In order to investigate this behavior, we consider a network of sparsely connected excitatory and inhibitory spiking neurons with noisy stimulus input. For sufficiently strong inhibition, its activity oscillates and, for stronger inhibition, the equally-inhibited excitatory cells fire in distinguishable and precise time windows. The implications for the encoding and decoding of stimuli are then discussed.

Key words: Olfaction, Antennal lobe, Oscillations, Synchronization, Coding
PACS: 87.19.La, 87.10.+e

1 Introduction

Electrophysiological measurements in the locust antennal lobe (AL), the analogue of the mammalian olfactory bulb for insects, have shown that, during odor stimulation, this network presents an oscillation around 20 Hz together with an odor-specific transient synchronization of the projection neurons (PNs) [5]. These findings suggest that odors could be encoded in the AL by assemblies of PNs firing quasi-synchronously. In the mushroom body, a higher brain structure, Kenyon cells (KCs) receive the AL input from a subset of about 10-20 PNs and for a given synchronized epoch in the AL, very few KCs fire [7]. These cells are thought detect the coincidence in the firing of

---

[*] Corresponding author.
  Email address: hugues@loria.fr (Etienne Hugues).

the PN subset. In spite of the fact that a biologically detailed model of the AL has reproduced the experimental observations [1], the AL dynamics is still insufficiently known to understand precisely how a stimulus is encoded in the PN population firing times.

In this paper we consider a simplified version of the spiking neural network proposed in [1]. We study its global behavior and the firing times of individual excitatory cells. Finally, we discuss the implications of these results on the encoding of stimuli.

2 The model

In this study, we want to describe general phenomena occuring in certain kinds of networks. However, as we refer to what happens in the insect AL, we only show simulations for parameter illustrating this structure. The model used here is a quite idealized version of the one proposed in [1] which uses conductance-based neurons. Nevertheless, our results remain qualitatively the same.

We consider a sparsely connected network of N_E excitatory (E) and N_I inhibitory (I) quadratic integrate-and-fire (QIF) neurons [4]. The dynamics of the neuron n in the population α ($\alpha = E, I$) is described by

$$\tau_\alpha \frac{dv_{\alpha n}}{dt} = v_{\alpha n}^2 + i_{\alpha n}^{app}(t) + i_{\alpha n}^{syn}(t) - i_\alpha^{th}, \tag{1}$$

where $v_{\alpha n}$ is the potential of the neuron, τ_α its membrane time constant, $i_{\alpha n}^{app}$ its applied external current due to the presence of the stimulus, $i_{\alpha n}^{syn}$ its synaptic current and i_α^{th} its threshold current. One important feature of the model is that E-cells are more excitable than I-cells, *i.e.* $i_I^{th} > i_E^{th}$ (> 0). When its potential diverges towards $+\infty$, the neuron emits a spike and its potential is immediately reset to $-\infty$ [1]. The synaptic current elicited by this spike is modeled by a decreasing exponential with time constant τ_α^s, and initial amplitude $g_{\alpha\beta}$ when the postsynaptic neuron belongs to the population β. The connectivity is random, with connexion probability p.

The class of stimuli we consider consists in choosing a subset of N_E^s E-cells and N_I^s I-cells and apply to them the current $i^{app}(t) = i + \sigma\eta(t)$ where $\eta(t)$ is a white noise with $< \eta(t)\eta(t') >= \delta(t - t')$ and σ is the noise amplitude. In the AL, this noisy input current comes from the convergence on each glomerulus of many olfactory receptor neurons spike trains. The other cells have no applied

---

[1] In the simulations, the equivalent non-diverging theta neuron has been used.

current. Another important feature of the model is that $i_E^{th} < i < i_I^{th}$, so that E-cells receiving the stimulus will have the natural tendency to fire and I-cells will fire when sufficiently excited by the E-cells.

As we will take $g_{EE} = 0$, E-cells which do not receive the stimulus cannot fire. In the following, we will consider that i_I^{th} is sufficiently high to prevent the I-cells which do not receive the stimulus to fire [2]. Under these conditions, only the cells receiving the stimulus will fire, the others having no role in the dynamics : thus, these cells will be discarded from the network, the stimulus being now represented in the number of remaining neurons and in the remaining connectivity.

In the following we will show simulations of the real scale locust AL which contains $N_E \approx 830$ and $N_I \approx 300$ (see [1,6] for the choice of the parameters) : $\tau_E = 4.5$ ms, $\tau_I = 2.6$ ms, $i_E^{th} = 0.5$, $i_I^{th} = 0.8$, $\tau_E^s = 5$ ms, $\tau_I^s = 10$ ms, $p = 0.05$, $g_{EI} = 0.1$, $g_{IE} = g_{II} = -0.5$. Stimuli are characterized by $i = 0.75$, $\sigma = 0.03$, $N_E^s = 0.75\,N^s$ and $N_I^s = 0.25\,N^s$, N^s being the number of stimulated neurons varying according to the number of stimulated glomeruli.

3   Network and neuronal dynamics

In order to understand the role of inhibition on the network dynamics the inhibition strength was varied, at fixed excitation g_{EI}, along a line defined by $(g_{IE}^x, g_{II}^x) = x\,(g_{IE}, g_{II})$ where $x > 0$. Independently of the choice of the network parameters, a typical behavior was observed. At weak x value, the network presents a non-oscillatory behavior or asynchronous state. Above a certain threshold x_{osc}, the network oscillates at a frequency f which slowly decays with N^s ($f \approx 20$ Hz for the AL parameters). Above and around this threshold, neurons can still fire at almost any time and both populations are not synchronized. A similar transition has been found theoretically in networks of integrate-and-fire neurons [3]. Due to the sparse random connectivity, different E-cells receive different numbers of projections from the I-cells. When x increases away from x_{osc}, neurons tend to synchronize their action potentials : the time at which a particular E-cell will fire depends on the number n of inhibitory inputs it has received at the preceding oscillatory cycle. A smooth transition occurs around a certain x_{pr} value, above which the firing of the E-cell population is divided into different quasi-synchronized clusters of cells which have received the same number of inhibitory inputs (see Fig. 1). Moreover, these clusters are ordered in time with increasing inhibition. The number of E-cells in these clusters is basically the same from one oscillatory cycle to the other, as is N_I^e, the number of emitting I-cells (see Fig. 2). This number

---

[2] This has been verified for the simulations shown below.

3

is theoretically given by $N_E^s P_{N_I^e,p}^{bin}(n)$ where $P_{N_I^e,p}^{bin}$ is the binomial distribution for N_I^e emitting I-cells and connection probability p, whose mean is $N_I^e p$ and standard deviation is $\sqrt{N_I^e p(1-p)}$. The simulation results compare very well with this distribution.
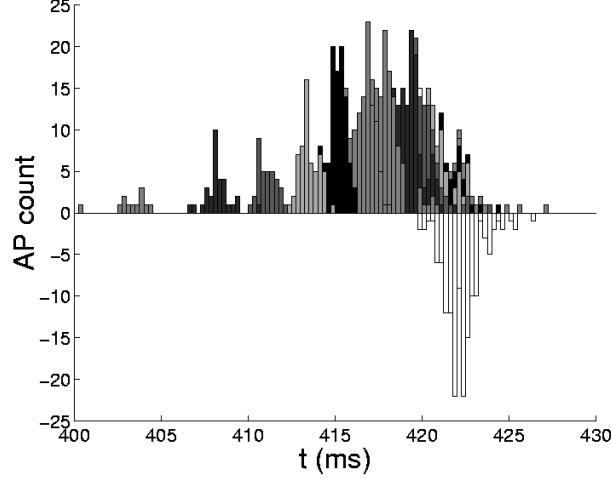

Fig. 1. Histogram of the E-cells (positive) and I-cells (negative) firing times for $N^s = 800$. The E-cells clusters receiving the same number of inhibitory inputs is indicated by a given grey level.

These clusters of E-cells that fire at precise times can be seen as encoding clusters. Actually, the identity of these neurons is determined by the I-cells that have fired at the preceding activity peak via the I $\rightarrow$ E connexions, and these I-cells have been verified to be uniquely dependent of the stimulus. Thus, the clusters of E-cells are stimulus-specific.
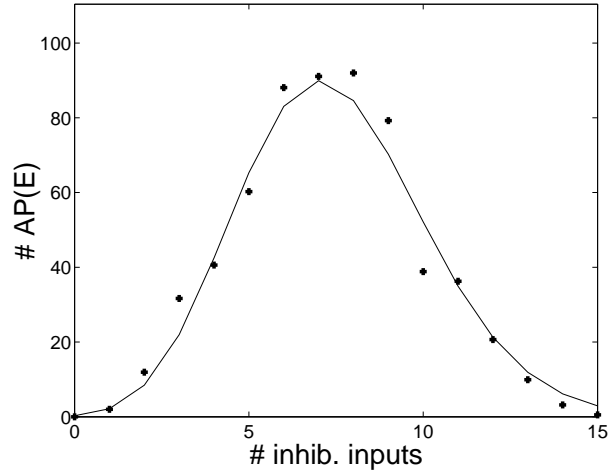

Fig. 2. Mean number of E-cells receiving a given number of inhibitory inputs for $N^s = 800$. The simulation results (*cross-marks*) are compared with the binomial distribution with $N_I^e = 150$ (*continuous line*).
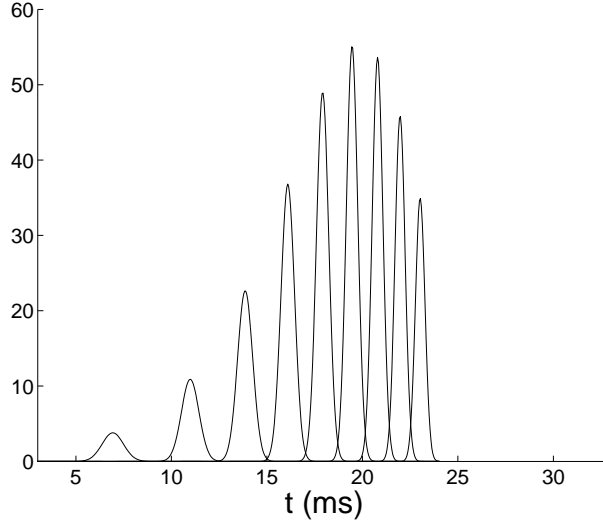
4

Fig. 3. Predicted distributions of the E-cells firing times when inhibited n times $(n = 2, ..., 10)$ by the I-cells.

The mechanism responsible of the observed neuronal clusters can be explained by considering individual neurons. Actually, when the neuronal populations are sufficiently synchronized, they form spike volleys of short duration. In this case, one E-cell receives quasi simultaneously a given number of inhibitory inputs -say n, which is, just after the I-cells spike volley, described by an exponential current. The same kind of situation has been studied in [2], where it was shown that a QIF subject to a strong inhibitory current of amplitude g tends to fire close to the time $T^*(g) \approx \tau_I^s \log g + T_0(i, \tau_I^s)$ whatever their initial potential is. The reason for this behavior is that, withoutr noise, two neighboring trajectories $v_E(t)$ and $v_E(t) + \delta v_E(t)$ get closer in time when $v_E < 0$ as δv_E obeys, when small, to the linearized equation $\tau_E \, d\delta v_E/dt = 2 \, v_E \, \delta v_E$, and this situation lasts longer for a higher inhibition. The cluster mean time, $T^*(n \, g_{IE})$, increases with n as $\tau_I^s \log n$. Furthermore, it can be shown that the cluster width, or standard deviation $\sigma_E(n)$, is related to the I-cells spike volley width or standard deviation σ_I by $\sigma_E(n) = \sigma_I/\sqrt{(n)}$. An example of predicted clusters is shown in Fig. 3.

The stimulus width N^s plays a role in the dynamics as it modulates the number of excitatory and inhibitory inputs to the neurons. Thus, the network capacity to encode a stimulus should depend on its width. Decreasing the width, one can see that the order of the E-cells clusters is still preserved, but these clusters are more spread. Moreover, they change from one oscillation to the other, till $N^s \approx 300$. Below $N^s \approx 300$, it appears that a large number of E-cells are not inhibited, and then fire at almost any time, decreasing the network synchrony. Therefore, this network is able to encode only stimuli that are large enough.

4   Discussion

We have seen that the firing of the E-cells is structured in time-ordered clusters of cells. Furthermore, several of them are distinct from the others and contain a greater number of cells than the number of PNs connected to a given KC. It can then be inferred that each of these distinguishable and significant clusters could define, via the AL to mushroom body connectivity, the KCs that fire. This conjectured encoding-decoding relationship will be further investigated in future work.

These clusters exist only for sufficiently distributed stimuli. Thus, the AL seems to play its role only for large dimensional entries. Furthermore, this could explain a perception threshold for example at low concentrations where fewer glomeruli are activated. We have also seen that the encoding clusters of E-cells are different for sufficiently different odor concentrations. Therefore different KCs could be actived for different concentrations of the same odor. This observation is coherent with recent experimental results [8].

References

[1] M. Bazhenov, M. Stopfer, M. Rabinovich, R. Huerta, H.D.I. Abarbanel, T.J. Sejnowski & G. Laurent (2001). Model of transient oscillatory synchronization in the locust antennal lobe. *Neuron* **30**: 553-567.

[2] C. Börgers & N. Kopell (2003). Synchronization in networks of excitatory and inhibitory neurons with sparse, random connectivity. *Neural Comput.* **15**: 509-538.

[3] N. Brunel (2000). Dynamics of sparsely connected networks of excitatory and inhibitory spiking neurons. *J. Comput. Neurosci.* **8**: 183-208.

[4] B. Ermentrout (1996). Type I membranes, phase resetting curves and synchrony. *Neural Comput.* **8**: 979-1001.

[5] G. Laurent, M. Wehr and H. Davidowitz (1996). Temporal representations of odors in an olfactory network. *J. Neurosci.* **16**: 3837-3847.

[6] D. Martinez and E. Hugues (2003). A spiking neural network model of the locust antennal lobe : towards neuromorphic electronic noses inspired from insect olfaction. NATO Advanced Research Workshop on "Electronic Noses/Sensors for Detection of Explosives", October 2003, Coventry, U.K.

[7] J. Perez-Orive, O. Mazor, G.C. Turner, S. Cassenaer, R.I. Wilson and G. Laurent (2002). *Science* **297**: 359-365.

[8] M. Stopfer, V. Jayaraman & G. Laurent (2003). Intensity versus identity coding in an olfactory system. *Neuron* **39**: 991-1004.